Next Materials 8 (2025) 100751

Contents lists available at ScienceDirect

Next Materials

journal homepage: www.sciencedirect.com/journal/next-materials

Research article

Reduced NiGraf: An effective hydrogenation catalyst of large applicative potential

Matteo Formenti [a,1], Rosaria Ciriminna [b,2], Cristina Della Pina [a,*,3], Mario Pagliaro [b,*,4]

[a] *Dipartimento di Chimica, Università degli Studi di Milano, via Golgi 19, Milano 20133, Italy*
[b] *Istituto per lo Studio dei Materiali Nanostrutturati, CNR, via U. La Malfa 153, Palermo 90146, Italy*

ARTICLE INFO

Keywords:
NiGraf
Metal organic alloy
Aniline
Nickel
Reduced graphene oxide

ABSTRACT

The reduced form of NiGraf, a newly developed metal organic alloy comprised of graphene oxide entrapped within Ni-based nanoparticles subsequently reduced with thiophene (RGO@Ni), shows remarkably stable selective activity in the complete reduction of nitrobenzene to aniline carried out in liquid-phase under ultramild conditions (35 °C, 10 % excess of hydrazine as reductant). These results are practically relevant because molecularly doped metals hold great applicative potential as new-generation solid catalysts, especially when the metal used to entrap organic species consists of low-cost and earth-abundant nickel.

1. Introduction

Widely employed by industry as a precursor for dyes, agrochemicals, acetaminophen (paracetamol), and methylene diphenyl diisocyanate, an intermediate in polyurethane manufacture, aniline (benzenamine) is globally manufactured at 7 million t/a rate. Demand is strong and production growing at 5.3 % compound annual growth rate [1]. The industrial process employs the heterogeneously catalyzed nitrobenzene (NB) hydrogenation carried out either in vapor phase or in liquid phase. In the vapor phase process NB is fed with hydrogen into a tubular reactor containing a supported Cu catalyst at 270–290 °C and 1–5 bar in the presence of a 9:1 (H_2:NB) excess of hydrogen [2]. In the liquid phase process, the capability for utilization of reaction heat (more than 500 kJ mol^{-1}) is much higher due to higher heat transfer coefficient, and supported noble metals (palladium and platinum) are employed [3].

Given the industrial and economic relevance of the process, plentiful academic and industrial research is still conducted today to improve the existing processes [4]. In 2005, Jackson in collaboration with catalysis industry's researchers demonstrated that the Haber's three-step reaction mechanism (aniline converted to nitrosobenzene, the latter to phenylhydroxylamine, and phenylhydroxylamine to aniline) is wrong [5]. The newly suggested reaction mechanism indicates formation of Ph–N(OH) as surface intermediate. In said mechanism, Ph–N(OH) either reacts with adsorbed hydrogen to form aniline, or Ph–N(OH) reacts with itself to eliminate water and produce azoxybenzene [5].

Ideally, hydrogenation of NB to aniline at completion would be carried out in liquid-phase at low temperature over a solid catalyst employing earth-abundant and low-cost Ni in place of Pt or Pd. So far, to the best of our knowledge, no such catalyst has been reported. Recently, for example, scholars in China reported a new Pt-loaded Ni@graphene magnetically separable catalyst (Pt/Ni@NG) at a Pt weight loading of 0.3 % exhibiting excellent activity for the hydrogenation of NB to aniline achieving a turnover frequency of 27,240 h^{-1} at 1 MPa reaction pressure and room temperature [6]. Remarkably, the catalyst retained its selective activity over five consecutive testing cycles. In another attempt, a catalyst comprised of 3.7 nm Ni nanoparticles dispersed on silica, though more active than Raney Ni, required 90 °C because formation of aniline only begins when the conversion of the strongly adsorbed nitrosobenzene intermediate is higher than 90 % [7].

In the following, we describe the high and stable activity in the NB reduction to aniline of the reduced form (RGO@Ni) of NiGraf, a newly developed metal organic alloy (MORAL) comprised of graphene oxide entrapped within Ni-based jamborite nanoparticles (GO@Ni) [8]. Actually consisting of jamborite nanoparticles encapsulating GO

---

[*] Corresponding authors.
E-mail addresses: cristina.dellapina@unimi.it (C. Della Pina), mario.pagliaro@cnr.it (M. Pagliaro).
[1] ORCID: 0000-0003-0580-0499.
[2] ORCID: 0000-0001-6596-1572.
[3] ORCID: 0000-0001-5628-0337.
[4] ORCID: 0000-0002-5096-329X.

https://doi.org/10.1016/j.nxmate.2025.100751
Received 10 March 2025; Received in revised form 6 May 2025; Accepted 23 May 2025

platelets [9], this new class of Ni-based catalysts is reproducibly and efficiently obtained through the MORAL approach first introduced by Avnir [10].

Since then, widely different molecularly doped metals were applied as enhanced catalysts to numerous catalytic conversions [11]. Yet, their uptake in catalysis science and technology in the subsequent two decades remained surprisingly low, even though metal species (organometallic compounds, nanoparticles and single-atoms) are by far the main catalytic species used in catalytic reactions [12]. Following the first entrapment of the graphene moiety in a metal lattice reporting the entrapment of GO in palladium metal nanoparticles [13], this study is the first to report the entrapment of graphene, in the form of RGO, in the metal-based nanoparticles by merging Avnir's route to molecularly doped metals [11], with GO reduction carried out with thiophene [14].

2. Experimental section

In detail, a 50 mL two-neck round bottom flask was added with 25 mL MeOH and 147 mg $NiCl_2•6H_2O$. (> 98 % purity, purchased from Fluka, Switzerland). Following dissolution of the nickel salt, the solution turned into bright green. The mixture was thus added with 0.111 mL of a GO aqueous suspension (8 mg/mL) purchased from Nanografi (Nanografi Nano Teknoloji, Istanbul, Turkyie). The mixture was sonicated using an ultrasound bath for 30 min. The reaction flask was then filled with N_2 gas at atmospheric pressure to create an inert atmosphere, followed by the addition under N_2 flow of 128 mg of $NaBH_4$ (purchased from Merck, > 96 % purity) (1:5 stoichiometric ratio). After about 30 min, the mixture was filtered through a Büchner filter and the filtrate extensively washed with Milli-Q water and MeOH. After drying at room temperature, a powder consisting of NiGraf (GO@Ni) deeply colored in black was obtained.

The material was characterized by Fourier Transform infrared spectroscopy (FTIR) using a JASCO FT/IR 4100 spectrometer (Jasco, Japan). A small sample of the catalyst was dispersed in highly pure KBr. The mixture was pressed under 10 t weight and the resulting pellet used to record the spectra in the 4000–400 cm^{-1} frequency range. The X-ray diffraction (XRD) pattern was measured using a Rigaku Miniflex 600 spectrometer (Rigaku, Japan) using the Cu Kα ($\lambda = 0.1541$ nm) radiation. Data were acquired in the 2θ range 10–80°. The scanning electron microscopy (SEM) photographs were taken using a SEM TM4000 PLUS II instrument (NanoVision, Japan) using an acceleration voltage of 15 kV. Samples were placed on a conductive carbon adhesive. Transmission electron microscopy (TEM) images were acquired on samples deposited on copper TEM grid with a carbon sept using a Thalos L120C instrument (Thermo Fischer Scientific, Waltham, MA, USA) operated at 120 kV.

RGO@Ni was readily obtained using thiophene (99 % pure, purchased from Sigma Aldrich) to reduce the GO in GO@Ni. After reduction, the RGO@Ni was extensively washed with methanol to remove oligo-olefins formed upon the rupture of the aromatic thiophene heterocycle. In detail, a 50 mL round bottom flask was added with 20 mL MeOH and 109 mg of GO@Ni under vigorous stirring. Nitrogen was fluxed in the flask to remove air, after which the mixture was added with 1 mL (12.48 mmol) of thiophene. The flask was immersed in a heating bath kept at 80 °C keeping the flask tightly closed in order to prevent solvent evaporation. After 24 h, stirring was stopped and the mixture cooled at ambient temperature followed by filtration through a Hirsch filter funnel followed by extensive washing with MeOH. Compared to GO@Ni, RGO@Ni is an even finer powder. This complicated the material recovery. To avoid material losses, thus, the mother liquor was filtered to recover any material losses through the filter. The catalyst was dried first under vacuum and then in open air at room temperature. The structure of the materials obtained was extensively characterized by different structural investigation techniques (XRD, SEM, TEM-EDS and FTIR).

3. Results and discussion

NiGraf (GO@Ni) was prepared as described elsewhere [8], and summarized by Eq. (1) (unbalanced). Its reduced version comprised of Ni-based nanoparticles doped with reduced graphene oxide (RGO@Ni), was prepared via partial reduction of graphene oxide with thiophene (Eq. (2), unbalanced).

$$NiCl_2 \cdot 6H_2O + GO \xrightarrow[r.t,\ 30\ min]{NaBH_4} GO@Ni \quad (1)$$

$$GO@Ni + C_4H_4S \xrightarrow[80^\circ C, 24\ h]{} RGO@Ni \quad (2)$$

3.1. Structural characterization

First reported by Lee and co-workers in 2013 as better alternative to conventional reduction of GO with hydrazine [13], reduction of GO with thiophene effectively reduces the oxidizable functions in GO. In the process thiophene is converted into oxidized thiophene polymer and then to polyhydrocarbon by loss of sulphur atoms. Evidence of successful GO reduction is obtained from the FTIR spectra of NiGraf (GO@Ni), reduced NiGraf (RGO@Ni) and GO in Fig. 1 In the spectrum of RGO@Ni in Fig. 1 the carboxylic C═O stretching signal at 1632 cm^{-1}, the carboxylic acid O-H stretching at 3400 cm^{-1}, and the C═O carbonyl signal at 1350 cm^{-1} evident in the spectrum of GO@Ni either disappeared or are very weak. Though weak, the stretching signal of graphene non-reduced C-O-C ether bonds at 1047 cm^{-1} is clearly present. This shows evidence that GO in the MORAL has been reduced to graphene (or reduced graphene oxide).

The XRD pattern of NiGraf in Fig. S1 (red curve) confirms that the MORAL is amorphous. However, overlap with the XRD profile of Ni and NiO shows that in the regions of the Ni and NiO diffraction peaks, the signal in the GO@Ni XRD pattern is enhanced. The XRD pattern of GO@Ni after employment of the material to mediate the nitrobenzene reduction with hydrazine in five consecutive catalytic runs (Fig. S2) shows a pattern even more similar to that of Ni, though remaining the diffraction pattern of an amorphous material.

The SEM photographs of GO@Ni in Fig. 2 show the high porosity of the NiGraf surface prior to reduction of GO with thiophene. The elemental mapping reveals that the distribution of Ni, C and O chemical elements within the sample is homogeneous, confirming that GO@Ni is comprised of GO entrapped within jamborite ($Ni(OH)_2(NiOOH)$) nanoparticles [8].

The XRD pattern of RGO@Ni (red curve), in Fig. 3 shows that RGO@Ni is an amorphous solid whose diffraction pattern shows enhanced peaks in proximity to the diffraction peaks of Ni and NiO.

The XRD profile of the same RGO@Ni material after five consecutive catalytic cycles in the reduction of nitrobenzene to aniline using

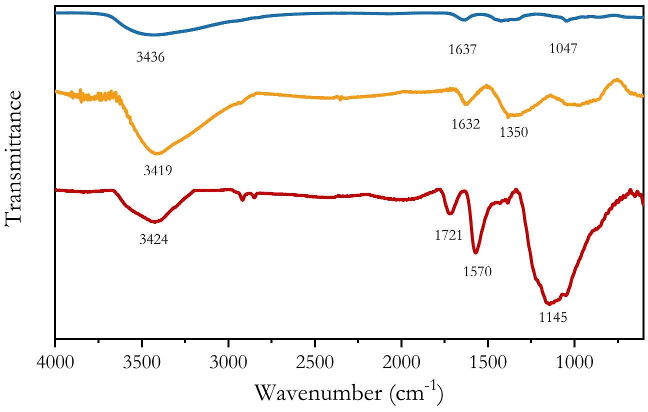

Fig. 1. FTIR spectra of GO (red), GO@Ni (yellow) and RGO@Ni (blue).

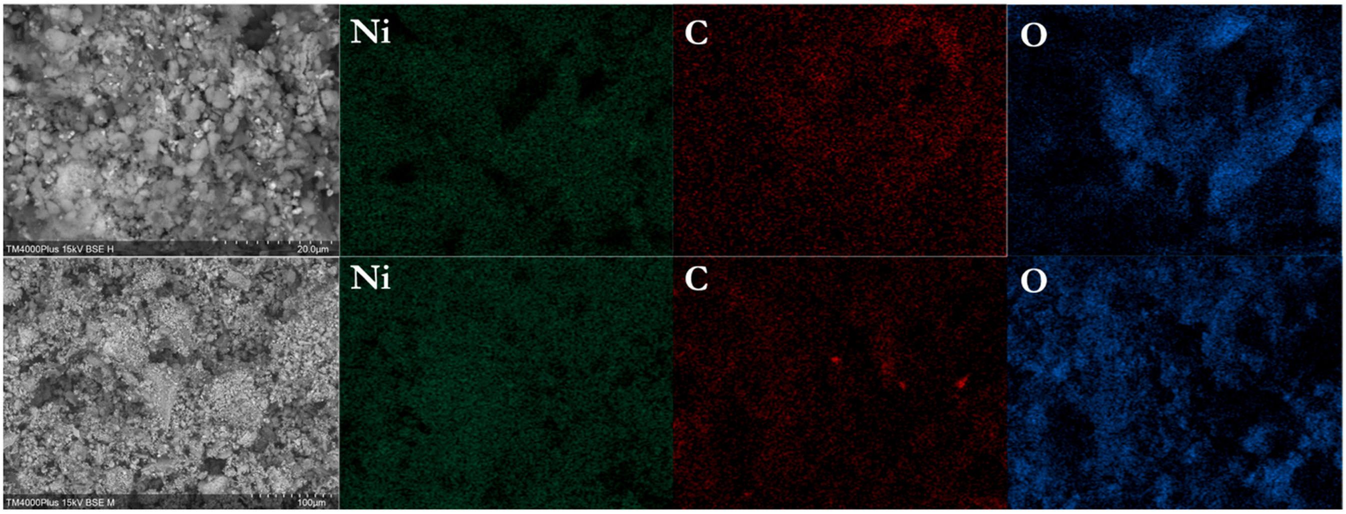

Fig. 2. SEM photographs and elemental maps of GO@Ni at different magnification levels.

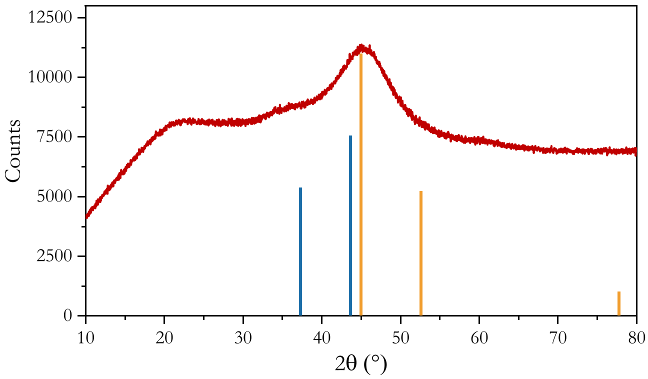

Fig. 3. XRD of RGO@Ni (red curve), Ni (yellow peaks) and NiO (blue peaks).

hydrazine as reductant in Fig. S3 shows that the material remains amorphous, though the aforementioned signals corresponding to Ni (yellow) and NiO (blue) are further enhanced.

We attempted to crystallize the structure of RGO@Ni metal-organic alloy by heating a sample of RGO@Ni under N_2 atmosphere at 200 °C for 2 h followed by slow cooling, in order to promote the growth of the crystal lattice driven by favored thermodynamics. The XRD pattern in Fig. S4 shows that partial re-crystallization took place. However, the MORAL remained substantially amorphous.

The TEM images at different magnification degrees in Fig. 4 show evidence that reduced NiGraf (RGO@Ni) consists of Ni agglomerates within which graphene layers are disorderly entrapped within the metal structure, and not wrapped around the Ni nanoparticles or regularly entrapped within said particles. The high-resolution TEM photograph in Fig. 5 shows a glassy graphene layered structure on the edge of the RGO@Ni metal-organic alloy.

Further evidence that RGO@Ni is amorphous is given by the diffraction pattern of the electron beam of the TEM instrument (Fig. S5). No circular diffraction pattern with well-defined peaks is observed, as it happens with crystalline materials, but rather concentric halos lacking any well-defined diffraction signal. The outcomes of the energy-dispersive X-ray spectroscopy (EDS) analysis conducted with the same TEM instrument show evidence (Fig. S6) that RGO@Ni chiefly consists of Ni (the copper signal is due to the copper mesh supporting the RGO@Ni sample).

Finally, the SEM photographs and elemental maps of RGO@Ni at different magnification levels in Fig. 6 show that reduction of GO to graphene using thiphene does not reduce the jamborite nanocrystals to Ni nanoparticles. Furthermore, the microphotographs confirm that reduction of GONi to RGO@Ni using thiphene retains the highly porous surface on the microscale of NiGraf, which is important for application

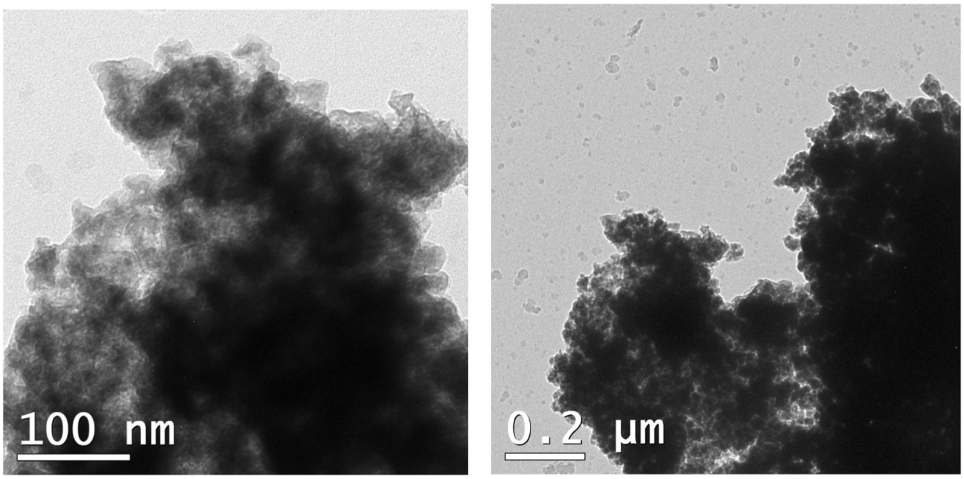

Fig. 4. TEM photographs of RGO@Ni at low magnification degrees.

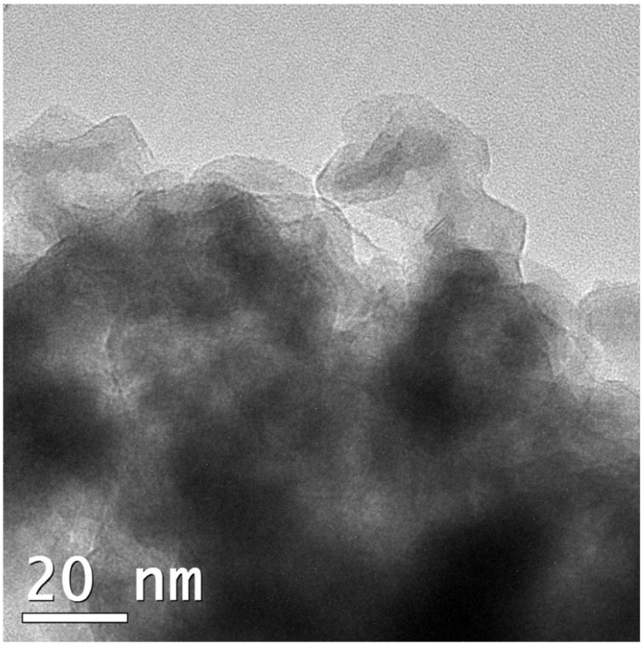

Fig. 5. High-resolution TEM photograph of RGO@Ni.

of this Ni-based family of MORALs in forthcoming heterogeneous catalytic reactions.

Both MORALs, GO@Ni and RGO@Ni, were employed in the reduction of nitrobenzene with hydrazine aimed at obtaining aniline.

3.2. Catalytic tests

We conducted numerous tests aimed at identifying the best reaction conditions for nitrobenzene reduction to aniline. In detail, reactions were conducted at 20, 35 and 50 °C. Reactions were conducted in MeOH and under biphasic conditions in water, either under static, regular atmosphere (air) or under N_2. Hydrazine was employed in 10 %, 40 %, 70 %, 100 % excess with respect to the hydrazine: NB = 1.5 stoichiometric ratio. Reaction times explored went from 24 h in the case of the reactions conducted at 20 °C, to 16 h for the reaction at 35 °C, and 4 h for the reactions at 50 °C. The optimal reaction conditions were: water as "on-solvent" reaction medium, inert atmosphere, 35 °C, reaction time of 230 min. Plots in Fig. 7 show both yield in aniline and substrate conversion for the reaction catalyzed by RGO@Ni under said optimal conditions.

Samples were withdrawn from $t = 0$ to $t = 230$ min when reaction was virtually complete. The suspension after 20 min was deeply colored in black due to the RGO@Ni catalyst dispersed in the aqueous mixture. After 40 min, the color turned into grey, due to formation of well-known NB reduction reaction intermediates. After 90 min the reaction mixture color turned into green due to the presence of relatively abundant amounts of azoxybenzene and azobenzene, as shown by the concomitant lowering of reaction yield in Fig. 7. After another 30 min, however, the green color started to vanish and after overall 200 min reaction time the reaction mixture was virtually devoid of any color showing evidence that all reaction intermediates were converted into aniline.

Histograms in Fig. 8 show evidence of the exceptional stability of the reduced NiGraf catalyst RGO@Ni, that entirely retains its selective activity in five consecutive reaction runs, affording full conversion of NB to aniline. NiGraf, on the other hand, shows dramatic drop in activity after the 3rd run, whereas nanoparticulate Ni loses activity already after the 2nd run. We hypothetically ascribe said enhanced stability to the electron donation of electrons in the valence band that extends over the whole sheet of graphene to empty d orbitals of Ni. Due to hybridization of the metal d-electrons with the π-orbitals of graphene, graphene and nickel strongly interact with graphene typically deposited on the surface of Ni [15]. 3D entrapment of graphene within the Ni metal lattice, however, is completely different from 2D surface adsorption, causing plentiful "side-contacts", namely contacts where Ni atoms interact with graphene edges, leading to formation of bonds between graphene-edges

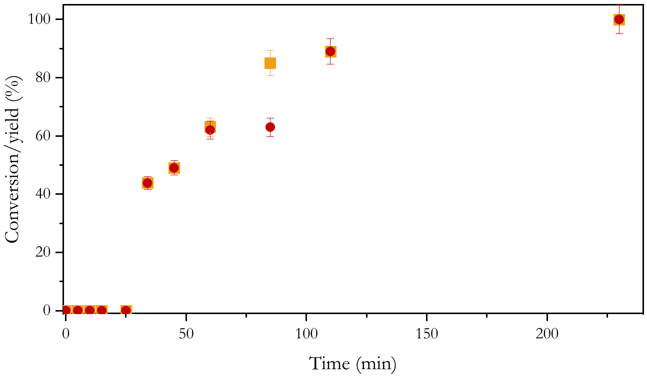

Fig. 7. Yield in aniline (red circles) and substrate conversion (yellow squares) in the reduction of nitrobenzene with hydrazine catalyzed by RGO@Ni (15 mol %) at 35 °C under N_2 atmosphere.

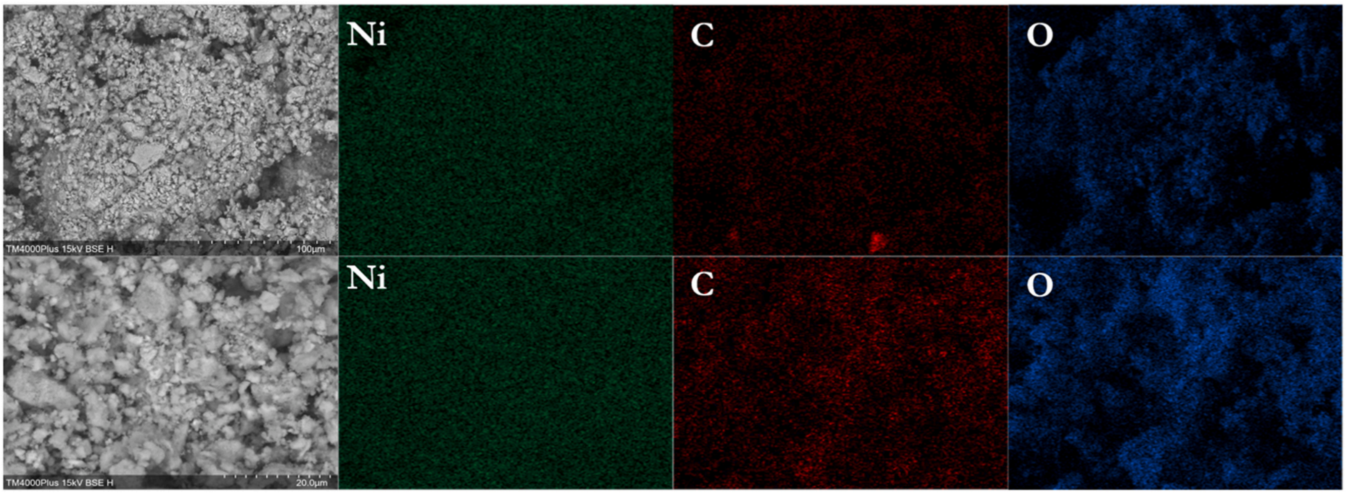

Fig. 6. SEM photographs and elemental maps of RGO@Ni at different magnification levels.

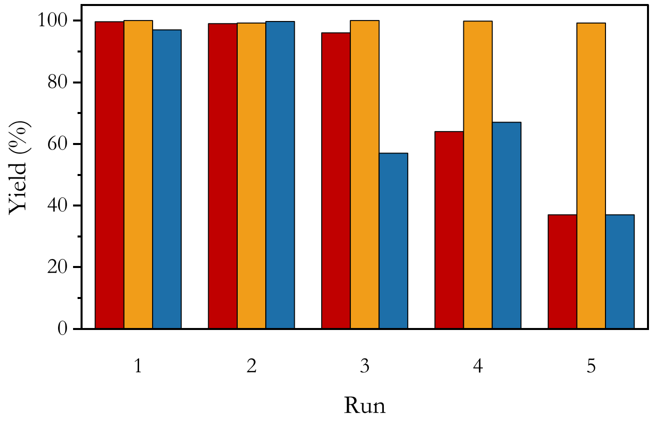

Fig. 8. Yield in aniline in the reduction of nitrobenzene to aniline with 10 % excess hydrazine catalyzed by GO@Ni (red, 15 mol%), RGO@Ni (yellow, 15 mol%) and Ni (blue, 15 mol%) at 20 °C under N_2 atmosphere.

and nickel [16]. The outcomes of density functional theory quantum chemistry calculations will be reported soon.

4. Conclusions

In conclusion, we have discovered that RGO@Ni, the reduced version of the new NiGraf catalyst comprised of reduced graphene oxide 3D entrapped within the lattice of Ni-based jamborite nanoparticles, has uniquely high stability in mediating the full reduction of nitrobenzene to aniline carried out in water only using a small (10 mol%) excess of hydrazine as reductant under remarkably mild conditions (35 °C and under N_2 atmosphere).

Besides having fundamental value, these results hold substantial applicative potential from the industrial viewpoint. Industry, indeed, has long been interested in identifying low-cost Ni-based heterogeneous catalyst for this important industrial process with which to replace expensive supported Pd or Pt catalysts in order to carry out the hydrogenation of NB in liquid phase that allows better heat dispersion and recovery [3]. The optimal reaction temperature of 35 °C for NB full conversion into aniline mediated by RGO@Ni, should be compared to the 90 °C required for its hydrogenation mediated, again in liquid phase, by Ni/SiO_2 [7]. Furthermore, the stability of the latter Ni nanoparticle-based catalysts is notoriously very low, with rapid leaching of nickel in solution and nanoparticle sintering and loss in activity, as shown also in the present work when employing powdered Ni catalyst.

It is also remarkable that the reaction readily takes place "on-water" under biphasic conditions, eliminating the need for any organic solvent, which may be relevant for laboratory-scale synthesis of aniline and hydrogenation of other nitroarene compounds, especially under continuous manufacturing conditions. In industrial applications, hydrazine will be replaced by H_2 and the reaction conducted under solvent-free conditions, dispersing the RGO@Ni powder in a large surface-area support as it is common in heterogeneous catalysts employed in industry.

Supplementary Information

Table S1: Results of the experiments aimed to optimize the reaction conditions. Fig. S3. XRD of RGO@Ni (red curve) after five consecutive catalytic cycles, Ni (yellow peaks) and NiO (blue peaks). Fig. S4. XRD profile of RGO@Ni upon heating up to 200 °C and slow cooling (red curve), Ni (yellow peaks) and NiO (blue peaks). Fig. S5. Electron diffraction pattern of RGO@Ni. Fig. S6. EDS analysis of RGO@Ni.

Declaration of Competing Interest

The authors declare that they have no known competing financial interests or personal relationships that could have appeared to influence the work reported in this paper.

Acknowledgements

We thank Università degli Studi di Milano for funding (PSR2023_DIP_005_PI_MSTUC). We thank Mario Orgnoni, undergraduate student at the University of Milan, for fruitful collaboration. We acknowledge Nicola Rotiroti from Unitech COSPECT, University of Milan (Italy), for performing TEM analyses. M.P. and R.C. thank the Ministero delle Imprese e del Made in Italy under the Piano Operativo della Ricerca "Ricerca e sviluppo sull'idrogeno" financially supported by the European Union—NextGenerationEU—M2C2 Investment 3.5, in the framework of the project PNRR Ricerca e Sviluppo sull'Idrogeno 2022–2025—Accordo di Programma "Idrogeno" (PRR.AP015.017.002), "Obiettivo 1—Produzione di idrogeno verde e pulito," "LA 1.1.6—Sviluppo di materiali e componenti non contenenti materiali critici per elettrolizzatori anionici (AEM) operanti anche ad elevata pressione differenziale".

Appendix A. Supporting information

Supplementary data associated with this article can be found in the online version at doi:10.1016/j.nxmate.2025.100751.

Data Availability Statement

Data supporting the findings of this study are available from the corresponding authors upon reasonable request.

References

[1] ChemAnalyst, Decode the future of aniline. New York, 2023. ⟨www.chemanalyst.com/industry-report/aniline-market-282⟩ (Accessed 19 February 2025).

[2] T. Kahl, K.W. Schröder, F.R. Lawrence, W.J. Marshall, H. Höke, R. Jäckh, Aniline, in: Ullmann's Encyclopedia of Industrial Chemistry, Wiley, New York, 2011.

[3] M. Turáková, T. Salmi, K. Eränen, J. Wärnå, D.Yu Murzin, M. Králik, Liquid phase hydrogenation of nitrobenzene, Appl. Catal. A: Gen. 499 (2015) 66–76, https://doi.org/10.1016/j.apcata.2015.04.002.

[4] M. Králik, M. Turáková, I. Mačák, P. Lehocký, Aniline – catalysis and chemical engineering. Proceedings of 41st International Conference of Slovak Society of Chemical Engineering, Tatranské Matliare, Slovakia, 2014, pp. 723–733.

[5] E.A. Gelder, S.D. Jackson, C.Martin Lok, The hydrogenation of nitrobenzene to aniline: a new mechanism, Chem. Commun. (2005) 522–524, https://doi.org/10.1039/b411603h.

[6] Y. Wu, Y. Si, Y. Huang, J. Diao, F. Meng, Z. Liu, H. Liu, Hydrogenation of nitrobenzene catalyzed by Pt supported on carbon coated nickel magnetic supports, Acta Metall. Sin. 60 (2024) 1141–1149, https://doi.org/10.11900/0412.1961.2024.00079.

[7] J. Wang, Z. Yuan, R. Nie, Z. Hou, X. Zheng, Hydrogenation of nitrobenzene to aniline over silica gel supported nickel catalysts, Ind. Eng. Chem. Res. 49 (2010) 4664–4669, https://doi.org/10.1021/ie1002069.

[8] M. Pagliaro, M.V. Pagliaro, R. Caliandro, C. Giannini, R. Ciriminna, A. Lavacchi, NiGraf: a new nickel-based molecularly doped metal for enhanced water electrolysis, Mater. Adv. 5 (2024) 2759–2766, https://doi.org/10.1039/d3ma00700f.

[9] R. Caliandro, E. Berretti, M.V. Pagliaro, R. Ciriminna, V. Mangini, C. Giannini, A. Lavacchi, M. Pagliaro, Structural dynamics of a nickel electrocatalyst during water splitting observed via operando pair distribution function, Cell Rep. Phys. Sci. 5 (2024) 102341, https://doi.org/10.1016/j.xcrp.2024.102341.

[10] H. Behar-Levy, D. Avnir, Entrapment of organic molecules within metals: dyes in silver, Chem. Mater. 14 (2002) 1736–1741, https://doi.org/10.1021/cm011558o.

[11] D. Avnir, Molecularly doped metals, Acc. Chem. Res. 47 (2014) 579–592, https://doi.org/10.1021/ar4001982.

[12] R. Ciriminna, M. Formenti, M. Pagliaro, C. Della Pina, Practical aspects concerning catalysis with molecularly doped metals, ChemCatChem 15 (2023) e202300600, https://doi.org/10.1002/cctc.202300600.

[13] M. Formenti, M. Pagliaro, C. Della Pina, R. Ciriminna, Graphene oxide in palladium nanoparticle (GrafeoPlad): a new class of functional materials, Green Synth. Catal, doi:10.1016/j.gresc.2024.04.004.

[14] S. Some, Y. Kim, Y. Yoon, H. Yoo, S. Lee, Y. Park, H. Lee, High-quality reduced graphene oxide by a dual-function chemical reduction and healing process, Sci. Rep. 3 (2013) 1929, https://doi.org/10.1038/srep01929.

[15] A. Dahal, M. Batzill, Graphene–nickel interfaces: a review, Nanoscale 6 (2014) 2548–2562, https://doi.org/10.1039/c3nr05279f.

[16] J. Lahiri, M. Batzill, Graphene destruction by metal-carbide formation: an approach for patterning of metal-supported graphene, Appl. Phys. Lett. 97 (2010) 023102, https://doi.org/10.1063/1.3464173.